arXiv:nucl-ex/9909009v1 15 Sep 1999

Vanishing spin alignment : experimental indication of triaxial $^{28}\mathrm{Si} + {}^{28}\mathrm{Si}$ nuclear molecule

R. Nouicer[1,*], C. Beck[1], R.M. Freeman[1], F. Haas[1], N. Aissaoui[1], T. Bellot[1], G. de France[1,†], D. Disdier[1], G. Duchêne[1], A. Elanique[1,3], A. Hachem[1], F. Hoellinger[1], D. Mahboub[1,3], V. Rauch[1], S.J. Sanders[4], A. Dummer[4], F.W. Prosser[4], A. Szanto de Toledo[2], Sl. Cavallaro[3], E. Uegaki[5] and Y. Abe[6]

[1] *IReS, UMR7500, CNRS-IN2P3 et Université Louis Pasteur, B.P.28, F-67037 Strasbourg, Cedex 2, France*

[2] *Instituto de Fisica da Universidade de São Paulo, São Paulo, Brazil*

[3] *Dipartimento di Fisica dell'Universitá di Catania, INFN and LNS Catania, Italy*

[4] *Department of Physics and Astronomy, University of Kansas, Lawrence, KS 66045, USA*

[5] *Department of Physics, Akita University, Akita 010, Japan*

[6] *Yukawa Institute for Theoretical Physics, Kyoto University, Kyoto, Japan*

(February 8, 2008)

---

[*] Present address: University of Illinois at Chicago and Argonne National Laboratory, IL 60439, USA.

[†] Present address: GANIL, Caen, France.

Abstract

Fragment-fragment-γ coincidences have been measured for ^{28}Si + ^{28}Si at an energy corresponding to the population of a conjectured resonance in ^{56}Ni. Fragment angular distributions as well as γ-ray angular correlations indicate that the spin orientations of the outgoing fragments are perpendicular to the orbital angular momentum. This differs from the ^{24}Mg + ^{24}Mg and the ^{12}C + ^{12}C resonances, and suggests two oblate ^{28}Si nuclei interacting in an equator-to-equator molecular configuration.

PACS numbers: 25.70.Ef, 23.20.En, 24.70.+z

In heavy-ion collisions the observations of unusual modes of nuclear excitations, such as giant dipole resonances built on excited states, scissors mode vibrations, and quasimolecular resonances, have led to important insights regarding nuclear and subnuclear degrees of freedom. Most of these special dynamical modes can be understood as collective oscillations around potential minima in the macroscopic nuclear potential energy surface. These minima, which may correspond to spherical, deformed, and superdeformed configurations of the composite system, can allow states which are sufficiently long-lived to strongly influence the dynamics of the system. The search for nuclear molecules has a long history [1] starting with the pionnering discovery [2] of the so-called quasimolecular resonances in the $^{12}\mathrm{C} + {}^{12}\mathrm{C}$ scattering in the Coulomb barrier region. Subsequently, intermediate width resonances were also discovered in the excitation functions of mutual inelastic $^{12}\mathrm{C} + {}^{12}\mathrm{C}$ scattering yields well above the Coulomb barrier [1,3]. These latter resonances were found to be associated with a mutually aligned component [3] suggestive of the formation of a rotating dinuclear complex in an equator-equator sticking configuration [4] because of the oblate shape of $^{12}\mathrm{C}$. The most intriguing evidence for such exotic excitation modes in dinuclear systems is the observation of pronounced, narrow, and well-isolated resonant structures in elastic and inelastic excitation functions measured for various medium-mass compound nuclei (CN) ($40 \leq A_{\mathrm{CN}} \leq 60$) [5,6]. The observation of resonant structures in the medium-mass region was first reported for the $^{28}\mathrm{Si} + {}^{28}\mathrm{Si}$ reaction [5], and subsequently for the $^{24}\mathrm{Mg} + {}^{24}\mathrm{Mg}$ reaction [6,7]. This resonant structure, strongly correlated in the exit channels, suggested a correspondance to quasimolecular states in $^{56}\mathrm{Ni}$ at high excitation energy ($E^{*}_{\mathrm{CN}} = 60$–$75\,\mathrm{MeV}$) and high angular momenta (34–$42\,\hbar$). These large values of angular momenta are of special interest because they exceed the rotating liquid drop model limit [7].

Based on the results of Nilsson-Strutinsky calculations, it has been suggested [8] that shell-stabilized superdeformed states may exist in the secondary minima of the adiabatic potential energy surfaces for the $^{56}\mathrm{Ni}$ nucleus in the region of high E^{*}_{CN} and large angular momenta relevant to the observed resonances. The $^{28}\mathrm{Si} + {}^{28}\mathrm{Si}$ resonances would then be associated with metastable quasimolecular configurations with extreme deformations. Spin alignment measurements [9,10] for the resonant $^{24}\mathrm{Mg} + {}^{24}\mathrm{Mg}$ system are already available. Based on these measurements, a deformed configuration is suggested for the $^{48}\mathrm{Cr}$ dinuclear system that corresponds to two prolate deformed $^{24}\mathrm{Mg}$ nuclei in a pole-to-pole arrangement [7]. Because of the complexity of the resonant structure, where several narrow resonances are found to have the same resonance spin, its analysis solely within a static approach is difficult. Dynamical aspects of this dinuclear complex were studied within a molecular approach [11,12]. Similar calculations have been applied for $^{28}\mathrm{Si}+{}^{28}\mathrm{Si}$ [13] which is, however, an axially nonsymmetric system arising from the oblate deformation of the $^{28}\mathrm{Si}$ nucleus in its ground state. To explore these differences and to obtain more precisely the triaxial properties of the $^{28}\mathrm{Si} + {}^{28}\mathrm{Si}$ resonances, we have performed a high-statistics experimental study of the $^{28}\mathrm{Si} + {}^{28}\mathrm{Si}$ collision at an energy corresponding to a conjectured $J^{\pi} = 38^{+}$ resonance in $^{56}\mathrm{Ni}$ [5].

In this Rapid Communication we report on experimental results obtained at the Strasbourg VIVITRON Tandem accelerator using a $^{28}\mathrm{Si}$ beam of energy $E_{\mathrm{lab}} = 111.6\,\mathrm{MeV}$. The analyzing magnet was calibrated before and after the experiment with a reproducibility of better than 0.07% to make sure that the chosen energy does well populate the resonance [5]. The beam struck a $25\,\mu\mathrm{g/cm}^2$ thick $^{\mathrm{nat}}\mathrm{Si}$ (92% of $^{28}\mathrm{Si}$) target. The Si target thickness corresponds to a beam energy loss of $\Delta E = 130\,\mathrm{keV}$, which is smaller than the width of the resonance ($\Gamma_{\mathrm{lab}} \approx 300\,\mathrm{keV}$). In order to check the beam energy, previous results of large-angle elastic scattering cross sections [14] available at close bombarding energies were compared with the present experiment. Heavy fragments were detected in coincidence using two large-area Si position-sensitive detectors located symmetrically on either side of the beam axis in order to cover the laboratory angular range from 22° to 73° in the horizontal plane with a solid angle of 114 msr and a vertical angular acceptance of $\approx \pm 4°$. The γ rays emitted from the fragments were detected in the 54 Compton-suppressed Germanium detectors of the EUROGAM PHASE II multidetector array. Data were taken in both double and triple coincidence modes : fragment-fragment (F-F) and fragment-fragment-γ (F-F-γ), respectively.

The excitation-energy (E_{x}) spectrum corrected for F-F detection efficiency in the ^{28}Si + ^{28}Si exit-channel is shown as histograms in Fig. 1. The cross sections have been obtained after integration over the range of scattering angles $61° \leq \theta^{\mathrm{FF}}_{\mathrm{c.m.}} \leq 114°$. The spectrum is dominated by peaks corresponding to transitions to large negative Q-values and to mutual inelastic excitations with large spins. For $E_{\mathrm{x}} \leq 10\,\mathrm{MeV}$ the identification of most of the states based on their γ decay is straightforward and spin assignments of the lowest energy peaks are given in the figure. Their peak yields are in very good agreement with previous elastic, 2^+, and (2^+,2^+) cross sections data [5,15] taken at the 38^+ resonance energy of $E_{\mathrm{lab}} = 112\,\mathrm{MeV}$. An analysis of the results of Ref. [14] taken at three bombarding energies 111, 112, and 113 MeV, which span the resonance in the same angular range $90° \pm 1.8°$, gives the ratios of the mutual to single 2^+ excitations as $\sigma(2^+, 2^+)/\sigma(2^+) = 1.45 \pm 0.01$, 1.64 ± 0.02 and 1.24 ± 0.01, respectively. The present data yield $\sigma(2^+, 2^+)/\sigma(2^+) = 1.65 \pm 0.01$ indicates that the VIVITRON beam energy chosen for this work was close to the resonance energy of 112 MeV. The dashed line in Fig. 1 shows the results of statistical-model calculations according to the transition-state model (TSM) for fission decay using standard parameters for ^{56}Ni CN [16]. At high excitation energies ($\mathrm{E}_{\mathrm{x}} \geq 10\,\mathrm{MeV}$), where the number of possible mutual excitations is large, the TSM calculations are in qualitative agreement with the data and suggest the importance of the fission decay in this energy region. For discrete low-lying states ($E_{\mathrm{x}} \leq 4\,\mathrm{MeV}$) a resonant, nonstatistical behavior is known to dominate the yields of these exit-channels and, consequently, as shown in Fig. 1, it is not surprising that the TSM calculations fail to describe these yields.

In order to investigate the resonant effects and to determine their most favorable angular momentum, we extracted the F-F angular distributions (AD) by selecting excitation energy ranges corresponding to different states of the two ^{28}Si fragments [17,18]. For the low-lying states, the various (elastic, 2^+, 2^+-2^+) exit-channels were found to display strongly oscillatory AD at backward angles in the center-of-mass (c.m.) range $68° \leq \theta^{\mathrm{FF}}_{\mathrm{c.m.}} \leq 111°$ as shown in Fig. 2. Although very weak at backward angles the elastic cross sections are some 2 to 3 orders of magnitude above optical model predictions [8]. The 2^+_1-2^+_1 group could not be resolved from the much weaker excited 4^+_1 level in the F-F data alone. However, the F-F-γ data were used to determine the position of the 4^+_1 state and to set a narrow 2^+_1-2^+_1 coincidence gate in Fig. 1 accordingly to minimize the 4^+_1 contribution [17,18]. The γ-ray efficiency corrected F-F-γ spectrum gated by the 4^+_1 to 2^+_1 γ-ray transition (E_γ = 2839 keV) [17] (shaded histograms) shows that only a very small fraction of the 2^+_1-2^+_1 peak (it can be estimated to be less than 5 %) correspond to a contribution of the 4^+_1 state in the F-F spectrum of Fig.1. Similarly narrow Q-value gates were chosen for the elastic and single 2^+ peaks (a Gaussian fit of the 2^+ peak would suggest a contribution of less than 6 % to the mutual peak). The regular oscillations are periodic and thus rather well described by the solid curves of Fig. 2 calculated with $[\mathrm{P}_{L=38}(\cos\theta)]^2$ (the dashed and dotted-dashed lines have been calculated with L=36 and L=40 respectively). Despite the possible contamination of more direct reaction mechanisms and the admixture of smaller angular momenta, $L = 38$ gives clearly a superior fit (at least for the elastic and single inelastic channels) in good agreement previous elastic measurements [5,14]. The 2_1^+-2_1^+ channel might also contain the contribution of $L = 36$ but the $L = 40$ cannot be completely ruled out either. The AD's measured for the four lowest energy states are consistent with AD results obtained at the resonance energy for the same channels [15]. The fact that the measured AD's correspond to shapes characterized by the same angular dependence indicates that the resonant behavior is favored by the partial wave associated with $L = 38\,\hbar$. Although this is not a firm spin assignment, it does suggest that this might be the spin value of the resonance in accordance with the previous claims [5,15]. Since the total angular momentum $\vec{J} = \vec{L} + \vec{S}$ (where $\vec{S}$ represents the total channel spin of the fragments) is conserved and $L = 38\,\hbar$ is the most favorable partial wave in the three resonant exit-channels, this implies that the projection of the fragment spins along the direction perpendicular to the reaction plane corresponding to the magnetic substate $m = 0$. For higher excitation energy $E_\mathrm{x} \geq 6\,\mathrm{MeV}$, the identification of the dominant excited states (4_1^+, 2_1^+) and (4_1^+, 4_1^+) shown in Fig. 1 was verified by using the F-F-γ data [17,18]. In Fig. 2, the AD for the mutual excitation states (4_1^+, 2_1^+) at an excitation energy $E_\mathrm{x} \approx 6.7\,\mathrm{MeV}$ is not as strongly structured as the AD for the low-lying states, whereas the AD for the mutual excited states (4_1^+, 4_1^+) has a shape comparable to $1/\sin\theta^{\mathrm{FF}}_{\mathrm{c.m.}}$ indicating that the major part of the yields might have a dominant statistical fission origin as predicted by the TSM predictions (see Fig. 1).

The following analysis is focussed on the F-F-γ data in the $^{28}\mathrm{Si} + {}^{28}\mathrm{Si}$ exit channel with both ^{28}Si fragments being detected in $\theta^{\mathrm{FF}}_{\mathrm{c.m.}} = 90^\circ \pm 7^\circ$ (see Fig. 2) with a very narrow coincident gate set on the 2_1^+-2_1^+ peak of Fig. 1. Three quantization axes have been defined as follows : (a) the beam axis, (b) the axis normal to the scattering plane, and (c) the axis perpendicular to (a) and (b) axes. Since the two ^{28}Si fragments are detected in the angular region $83^\circ \leq \theta^{\mathrm{FF}}_{\mathrm{c.m.}} \leq 97^\circ$, the (c) axis corresponds approximately to the molecular axis of the out-going binary fragments. The experimental results of the γ-ray angular correlation $W(\theta_\gamma)$ (the polar θ_γ and azimuthal ϕ_γ angles being defined relatively to each of the quantization axes) for the 2_1^+-2_1^+ exit-channel are shown in Fig. 3 by points. The mutual excitation channel is here presented rather than the single excitation channel since it is known to induce more spin alignment in resonant systems such as $^{12}\mathrm{C} + {}^{12}\mathrm{C}$ [3] and $^{24}\mathrm{Mg} + {}^{24}\mathrm{Mg}$ [10]. The analysis method of the $W(\theta_\gamma)$ data is described in Ref. [7], in which the process of integration over ϕ_γ requires, due to the geometry of the EUROGAM spectrometer, some averaging over θ_γ. Our experimental efficiency for F-F-γ-γ detection is low and, consequently, the analysis was done with the condition of a γ multiplicity equal to one. The strong minimum in (b) at 90° implies $m = 0$ (see the following discussion) and thus that the intrinsic spin vectors of the 2^+ states are oriented in the reaction plane perpendicularly to the orbital angular momentum. The value of the total orbital angular momentum therefore remains close to $L = 38\,\hbar$, in good agreement with the AD results. The 4π geometry of the γ-ray spectrometer also allowed us to fit the $W(\theta_\gamma)$ (see Fig. 3, solid curve) to obtain more quantitative information about the contributions from the different magnetic substates (see Table I). As proposed in [7], the $W(\theta_\gamma)$ data have been described by an expression of the form $W(\theta_\gamma) = \sum_m P_m W_m(\theta_\gamma)$, where P_m represent either the magnetic substate population parameters in single or mutual 2^+ inelastic scattering, or the relative intensities of transitions with different Δm for E2 transitions between higher excited states. Since the parameters P_m enter the expression as linear coefficients of the pure-Δm functions $W_{\Delta m}(\theta_\gamma)$, the fits were calculated using a simple linear least squares procedure [7]. The fit values given in Table I show a significant *m=0* substate population, favored for both quantization axes (a) and (b) but not in (c), consistent with the spin vectors oriented in the reaction plane perpendicularly to the total angular momentum. The significant contributions of m = ± 2 are consistent with the AD analysis of the 2^+_1-2^+_1 which contain contributions from L=36 and 40. Admixtures of these other smaller orientations do not affect the observation of the dominant "disalignment" component consistent with the AD results.

The present AD and $W(\theta_\gamma)$ results are in contrast with the alignment found for the ^{24}Mg+ ^{24}Mg reaction [9,10]. The reason why the two systems differ so strongly may be associated with the structure of the dinucleus configuration. In $^{24}\mathrm{Mg} + {}^{24}\mathrm{Mg}$, the energetically favored configuration is the pole-to-pole configuration (see Fig. 1 of Ref. [12]) due to the prolate shape of ^{24}Mg. The system rotates about a minor axis of the ^{24}Mg nuclei (perpendicular to the symmetry axis). Therefore, the total angular momentum is parallel to the ^{24}Mg spins to give rise to alignment. The energetically favored configuration of an oblate-oblate dinuclear system is the equator-equator configuration (see Fig. 1 of Ref. [13]), with two pancakes touching each other side-to-side (^{28}Si is oblate in its ground state and the feeding of the bands of ^{28}Si has revealed that this nucleus is dominated by states with *oblate* deformation [17,18]). At a given angular momentum J, this configuration rotates in a triaxial way approximately about the axis normal to the plane defined by the two pancake-like nuclei which corresponds to the largest moment of inertia in the state with the lowest energy [19]. The spins of the ^{28}Si fragments are thus in this plane (m=0) since no rotation can occur about their symmetry axes. This analysis is consistent with the conclusions obtained from the analysis of the AD data. The molecular-model calculations [13] have been developed [19] to take into account the fact that the largest moment of inertia I_x is only slightly larger than the moment of inertia I_y about the in-plane axis that is perpendicular to the relative vector. This means that the total system is slightly axial asymmetric about the z-axis and therefore, the angular momentum vector is not completely parallel to the x-axis. To obtain an accurate description of this triaxial rotor, as it is wellknown for polyatomic molecules, we diagonalize the Hamiltonian of an asymmetric inertia tensor, which gives rise to a mixing of the K projections of the total spin J. In the high-spin limit ($K/J \approx 0$), the diagonalization is found to be equivalent to solving a differential equation of the harmonic oscillator with parameters given by the moment of inertia [19,20]. With the wave function obtained for the lowest energy state we have calculated the P_m's (given in Table I) as well as the $W(\theta_\gamma)$ (dashed lines) for the mutual inelastic channel (for which the second unobserved γ-ray is summed over all possible directions) which are compared with the data in Fig. 3. The characteristic features of the experiment (points) are in agreement with the molecular-model predictions [19]. A similar theoretical investigation was independently proposed to describe the $^{12}\mathrm{C} + {}^{12}\mathrm{C}$ scattering as an oblate-oblate dinuclear system in equator-equator orientations [4]. Although other possible pictures might be equally consistent to explain both the ^{28}Si$+$^{28}Si and ^{24}Mg$+$^{24}Mg scatterings, the present data will put severe constraints on future attempts with alternate model descriptions, such as, the double resonance model [21] or other coupled channel calculations [22].

In summary, the present high-resolution study of fragment-fragment-γ coincidence data collected with a powerful 4π γ-ray spectrometer for ^{28}Si $+$ ^{28}Si at $E_{\mathrm{lab}} = 111.6\,\mathrm{MeV}$, populating a well known molecular resonance in ^{56}Ni, does not show as strong evidence of fragment spin alignment with respect to the orbital angular momentum as found previously for ^{12}C $+$ ^{12}C and ^{24}Mg $+$ ^{24}Mg. This was first deduced from the measured fragment-fragment angular distributions of the elastic 0_1^+, inelastic 2_1^+, and mutual inelastic 2_1^+-2_1^+ channels, which appear to be rather well described by a partial wave with $L = 38\,\hbar$, and was confirmed by the analysis of the fragment-fragment-γ angular correlations for the mutual inelastic channel. These observations different from that of a spin alignment evidenced for ^{24}Mg $+$ ^{24}Mg resonances may support the occurence, predicted by the molecular model, of a stable ^{28}Si $+$ ^{28}Si oblate-oblate dinuclear system in which the equator-equator spin orientations result from its triaxial configuration. Similar high-statistics exclusive measurements at energies which do not correspond to a molecular resonance would be very instructive.

We are pleased to thank the VIVITRON operators and the EUROGAM staff of IReS. R. R. Betts and A. H. Wuosmaa are warmly acknowledged for a careful reading of the manuscript. This work was sponsored by the C.N.R.S. within CNRS/NSF and CNRS/CNPq Collaboration programs and also in part by the U.S. DOE under Grant No. DE-FG03-96ER40481.

REFERENCES

[1] R.R. Betts and A.H. Wuosmaa, Rep. Prog. Phys. **60**, 819 (1997), and references therein.
[2] D.A. Bromley, J.A. Kuehner and E. Almquist, Phys. Rev. Lett. **4**, 365 (1960).
[3] D. Konnerth *et al.,* Phys. Rev. Lett. **55**, 588 (1985).
[4] J. Schmidt and W. Scheid, Phys. Rev. C **53**, 322 (1996).
[5] R.R. Betts *et al.,* Phys. Rev. Lett. **47**, 23 (1981).
[6] R. Zurmühle *et al.,* Phys. Lett. B **129**, 384 (1984).
[7] A.H. Wuosmaa *et al.,* Phys. Rev. C **41**, 2666 (1990).
[8] R.R. Betts, Nucl. Phys. **A447**, 257c (1985).
[9] A.H. Wuosmaa *et al.,* Phys. Rev. Lett. **58**, 1312 (1987).
[10] A. Mattis *et al.,* Phys. Lett. B **191**, 328 (1987).
[11] R. Maass and W. Scheid, Phys. Lett. B **202**, 26 (1988).
[12] E. Uegaki and Y. Abe, Phys. Lett. B **231**, 28 (1989).
[13] E. Uegaki and Y. Abe, Phys. Lett. B **340**, 143 (1994).
[14] S.B. DiCenzo, Ph.D. Thesis, Yale University, 1980.
[15] R.R. Betts, private communication.
[16] S.J. Sanders, A. Szanto de Toledo and C. Beck, Phys. Rep. **311**, 487 (1999).
[17] R. Nouicer *et al.,* Heavy Ion Physics (World Scientific, Singapore, 1998), p. 538.
[18] C. Beck, Acta Phys. Pol. B **30**, 1527 (1999).
[19] E. Uegaki and Y. Abe, unpublished.
[20] A. Bohr and B.R. Mottelson, Nuclear Structure (Benjamin, New York, 1975) **vol. II**, p.175.
[21] K. Langanke *et al.,* Phys. Lett. B **112**, 116 (1982).
[22] A. Thiel *et al.,* Phys. Rev. C **29**, 864 (1984).

TABLES

TABLE I. Magnetic substate population parameters deduced from fits corresponding to each quantization axis of Fig. 3 and from the model predictions discussed in the text.

Quantization axis	$P_{m=0}$		$\mathrm{P}_{m=\pm1}$		$\mathrm{P}_{m=\pm2}$	
	Fit	Model	Fit	Model	Fit	Model
(a)	0.30 ± 0.08	0.48	0.16 ± 0.04	0.17	0.18 ± 0.05	0.09
(b)	0.46 ± 0.05	0.48	0	0	0.27 ± 0.02	0.26
(c)	0.14 ± 0.05	0.02	0.17 ± 0.03	0.17	0.26 ± 0.04	0.32

FIGURES

FIG. 1. Excitation-energy spectra for the ^{28}Si + ^{28}Si exit-channel in the angular region $61^\circ \leq \theta^{\rm FF}_{\rm c.m.} \leq 114^\circ$. The efficiency corrected F-F data (histograms) and the TSM calculations (dashed line) are integrated cross sections. The γ-ray efficiency corrected F-F-γ spectrum gated by the 2839 keV ($4^+ \rightarrow 2^+$) γ-ray transition is presented as shaded histograms.

FIG. 2. Experimental F-F AD of the elastic ($E_{\rm X} \approx 0\,{\rm MeV}$), inelastic ($E_{\rm X} \approx 1.7\,{\rm MeV}$), mutual inelastic ($E_{\rm X} \approx 3.6\,{\rm MeV}$) and higher excitations ($E_{\rm X} \approx 6.7$ and $9.7\,{\rm MeV}$). The dashed, solid, and dotted-dashed curves represent squared Legendre polynomials with $L = 36$, 38, and 40 respectively. The dotted curve corresponds to a $1/\sin\theta^{\rm FF}_{\rm c.m.}$ behavior.

FIG. 3. Experimental F-F-γ angular correlations of the mutual inelastic channel (2^+_1, 2^+_1) in the angular region $83^\circ \leq \theta^{\rm FF}_{\rm c.m.} \leq 97^\circ$ for the three quantization axes defined in the text. The solid and dashed curves are fits of the data and model predictions, respectively.

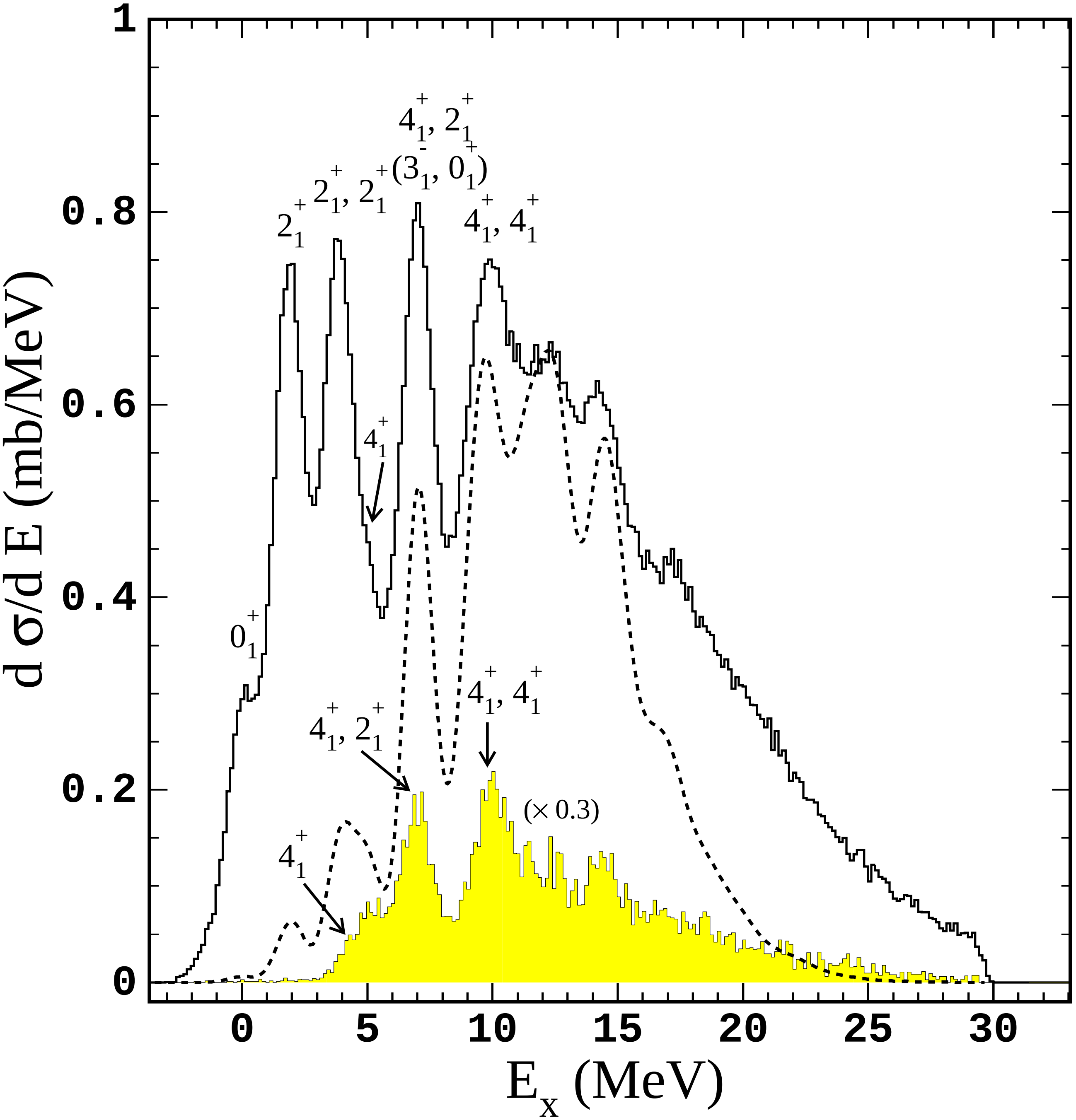
1
0.8
0.6
0.4
0.2
0
d σ/d E (mb/MeV)
0
5
10
15
20
25
30
E_x (MeV)
$4_1^+, 2_1^+$
$2_1^+, 2_1^+(3_1^-, 0_1^+)$
2_1^+
$4_1^+, 4_1^+$
4_1^+
0_1^+
$4_1^+, 4_1^+$
$4_1^+, 2_1^+$
(× 0.3)
4_1^+

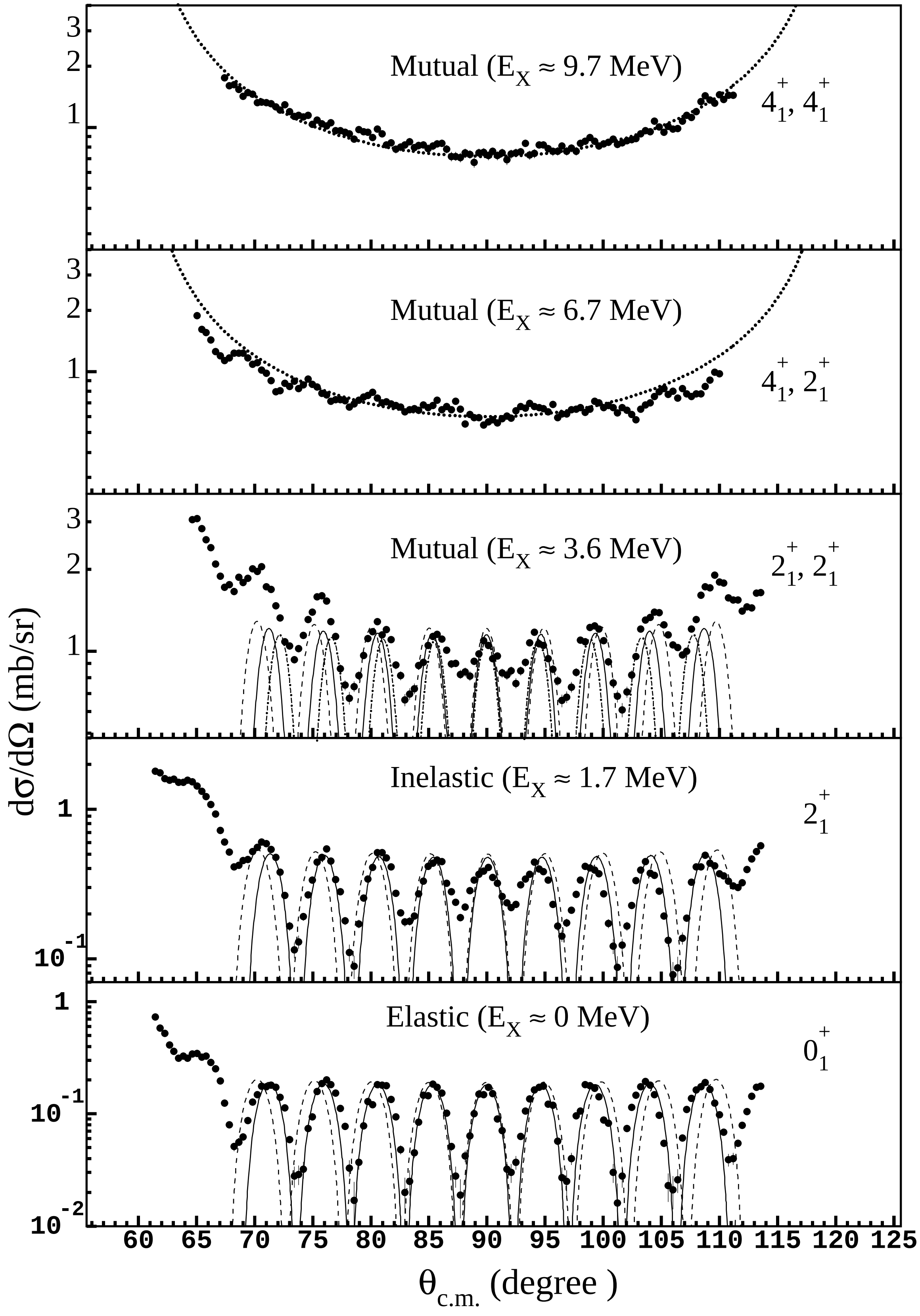

Mutual (E$_X$ ≈ 9.7 MeV)
$4_1^+, 4_1^+$
Mutual (E$_X$ ≈ 6.7 MeV)
$4_1^+, 2_1^+$
Mutual (E$_X$ ≈ 3.6 MeV)
$2_1^+, 2_1^+$
Inelastic (E$_X$ ≈ 1.7 MeV)
2_1^+
Elastic (E$_X$ ≈ 0 MeV)
0_1^+
dσ/dΩ (mb/sr)
θ$_{c.m.}$ (degree)
1
2
3
10^{-1}
10^{-2}
60
65
70
75
80
85
90
95
100
105
110
115
120
125

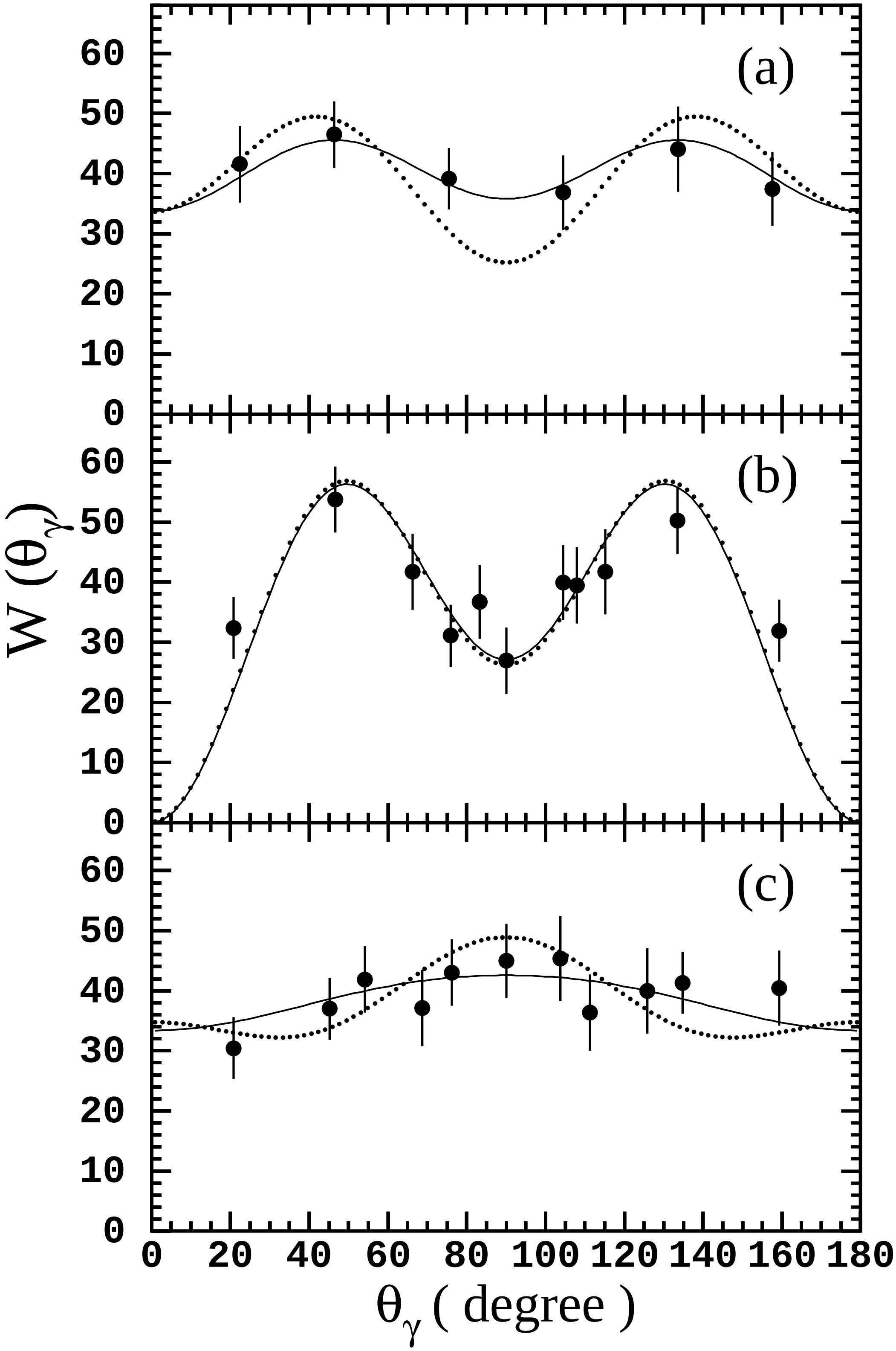
(a)
(b)
(c)
W (θ$_\gamma$)
θ$_\gamma$ (degree)
0
10
20
30
40
50
60
0
20
40
60
80
100
120
140
160
180